

# PCCP

Accepted Manuscript



This is an *Accepted Manuscript*, which has been through the Royal Society of Chemistry peer review process and has been accepted for publication.

*Accepted Manuscripts* are published online shortly after acceptance, before technical editing, formatting and proof reading. Using this free service, authors can make their results available to the community, in citable form, before we publish the edited article. We will replace this *Accepted Manuscript* with the edited and formatted *Advance Article* as soon as it is available.

You can find more information about *Accepted Manuscripts* in the [Information for Authors](#).

Please note that technical editing may introduce minor changes to the text and/or graphics, which may alter content. The journal's standard [Terms & Conditions](#) and the [Ethical guidelines](#) still apply. In no event shall the Royal Society of Chemistry be held responsible for any errors or omissions in this *Accepted Manuscript* or any consequences arising from the use of any information it contains.



PCCP

COMMUNICATION

## Ordered Ionic Liquid Structure Observed at Terraced Graphite Interfaces†

Received 00th January 20xx,  
Accepted 00th January 20xx

Xing He,‡ Chengyi Wu,‡ Karjini Rajagopal, Napat Punpongjareorn, and Ding-Shyue Yang\*

DOI: 10.1039/x0xx00000x

www.rsc.org/pccp

**Reflection high-energy electron diffraction is presented as a contactless, surface-specific method to probe the ion organization and layering at the ionic liquid-solid interfaces. Three regimes can be identified for the structure of 1-ethyl-3-methylimidazolium bis(trifluoromethylsulfonyl)imide ([EMIM][Tf<sub>2</sub>N]) on highly oriented pyrolytic graphite, which is strongly dependent on the distances of ions from the surface. Direct observations showed that the ultrathin ionic liquid (IL) assembly can exhibit the bulk-like phase-transition behaviors as a result of the structural matching between the IL and graphite layers and the confinement template effect due to the surface topography of graphite. The present study illustrates the opportunities for further studies of the structures and ultrafast dynamics of IL-solid interfaces.**

In the last two decades, room-temperature ionic liquids (ILs) have attracted great interest in various research communities and industries due to their remarkable physicochemical properties.<sup>1, 2</sup> Recently, more attention has been drawn to interfacial IL structures because of IL applications in, e.g., catalysis, electrochemistry, fuel cells, corrosion inhibition, and thin-film lubrication.<sup>3-5</sup> At the heart of these diverse phenomena, the structures, dynamics, and chemical reactivity at the heterogeneous interfaces are the determining factors. Ions and materials may exhibit unique or drastically different behaviours at nanometre-scale interfaces compared to their bulk properties in homogeneous phases. It is therefore essential to probe, with pertinent spatiotemporal resolutions, the interfacial structures and dynamics involved, with the former properties at equilibrium giving the basic picture at the molecular level.

To obtain signals pertaining to the IL-solid interfaces instead of the bulk ones, it is desirable to use methods whose probes are highly surface-sensitive or surface-specific. Such techniques include sum-frequency generation spectroscopy,<sup>4</sup>

x-ray reflectivity,<sup>6-8</sup> x-ray photoelectron spectroscopy (XPS),<sup>3, 9</sup> atomic force microscopy (AFM),<sup>5, 10, 11</sup> scanning tunnelling microscopy (STM),<sup>12, 13</sup> etc. However, considerable questions about the ion organization and layered structures still exist in the experimental literature.<sup>4, 5</sup> This might be due in part to the different situations that are inherent to different methods for probing the interfacial structures: force-dependent observations in AFM, the tip stability and ion adsorption in STM, beam-induced changes or damages by long exposure of x-ray, and averaged behaviours using optical techniques. A converging picture can be better reached if more data are collected by different techniques and cross-examined.

Our method of choice to probe the structures of IL-solid interfaces is reflection high-energy electron diffraction (RHEED), which can be modified and operated in a pulsed mode for studies of ultrafast interfacial dynamics.<sup>14, 15</sup> Compared to x-ray photons, electrons have orders-of-magnitude higher scattering cross sections with matter, can be easily generated and manipulated, and are less damaging to specimens per useful elastic scattering event.<sup>16</sup> These advantages make electrons a good choice of *contactless* probe for interfacial studies, with surface specificity of the order of 1 nm or less in the reflection geometry. Furthermore, the RHEED method allows visualization of the organization of ions through reciprocal-space imaging, which provides information about the order and disorder and phase transitions in interfacial molecular assemblies. Thanks to the nonvolatile property of ILs at room and low temperatures, ultrathin IL films prepared via physical vapour deposition<sup>9</sup> can be studied using RHEED under clean ultrahigh vacuum conditions, to exclude any potential effects of ordering/disordering caused by wetting or evaporation of a molecular solvent,<sup>10</sup> impurities, or ambient molecules (see ESI for experimental details†).

Here, we report the direct observation of an ordered IL structure on the surface of highly oriented pyrolytic graphite (HOPG) as a result of the lattice-matching template effect.<sup>15</sup> The IL of 1-ethyl-3-methylimidazolium bis(trifluoromethylsulfonyl)imide, [EMIM][Tf<sub>2</sub>N], was selected based on the considerations of its thermal stability for physical vapour

Department of Chemistry, University of Houston, Houston, Texas 77204, United States. E-mail: yang@uh.edu; Tel: +1 713 743 6022

† Electronic Supplementary Information (ESI) available: Additional figures and experimental details. See DOI: 10.1039/x0xx00000x

‡ These authors contributed equally.

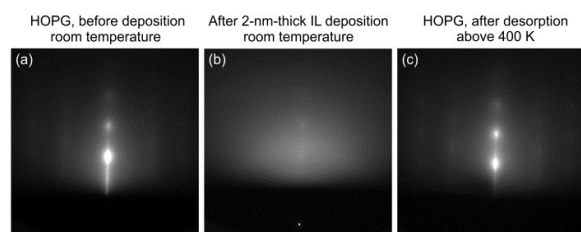


**Fig. 1.** RHEED images of the IL-HOPG interface. (a) The Bragg spots and vertical streaks from the HOPG substrate at room temperature before the IL deposition. (b) The diffuse scattering pattern recorded at room temperature after the deposition of a 2-nm-thick IL film on HOPG. The vague Bragg spots indicates that only an insignificant portion of the electron beam can penetrate the ultrathin IL film and produce weak diffractions from the substrate; a thicker film will fully block the HOPG features. (c) The recovered diffraction image of the HOPG substrate after complete desorption of the IL film at high temperatures.

deposition<sup>17, 18</sup> and the comparable sizes of the cation and the anion for potential packing orders in ultrathin interfacial assemblies. By changing the deposition time, IL films of <1 up to tens of nanometre (nm) in thickness were deposited on the surfaces of HOPG and monolayer graphene supported on 90-nm SiO<sub>2</sub>. Figure 1 shows the typical diffraction images of the IL-solid interfaces, using HOPG as an example. An adsorbate-free substrate surface can be fully recovered after complete desorption of the IL above 380 to 420 K, depending on the film thickness (Fig. 1, a and c); the clean surface was further confirmed to be free of the IL by XPS measurements and the absence of signals for N, F, and S atoms. We found that all of the nm-thick films deposited on the substrates held at room temperature yield a diffuse scattering pattern (with faint radial bands that correspond to the average intermolecular distances), without clear Bragg spots or Debye-Scherrer rings before cooling (Fig. 1b). Such an observation signifies the poor vertical and horizontal, or local, ordering of cations and anions at the IL-solid interface at room temperature when the surface is neutral. The best description for the general ion organization in these ultrathin IL films may be a *liquid-like* configuration (relative to a crystal structure) without extensive domains of a crystalline order or a polycrystalline nature.<sup>55</sup>

It is remarkable that the IL-HOPG interfaces readily produce clear Bragg diffractions, especially those equally spaced spots in the central streak, when the specimen temperature is sufficiently lowered (Fig. 2a). Such an observation was reproduced for more than 10 times when the film thicknesses were in the range of about 3 to 10 nm. These intense Bragg spots unequivocally indicate a good structural order along the surface normal direction (Fig. 2b). In addition to the intense ones, other diffractions, though much weaker in intensity, are also visible and aligned vertically and horizontally in the diffraction image, with well-defined spacing between the innermost vertical streaks (Fig. 2a, inset, and Fig. 2c). Based on the observed pattern, it is clear that the IL forms a good 3-dimensional crystalline order in the ultrathin film at low temperatures on the HOPG surface.

From the momentum transfer  $|\vec{s}| = (2/\lambda) \cdot \sin(\theta/2)$ , where  $\lambda = 0.07 \text{ \AA}$  is the wavelength of the probe electrons and  $\theta$  is the total scattering angle, it was found that the equal

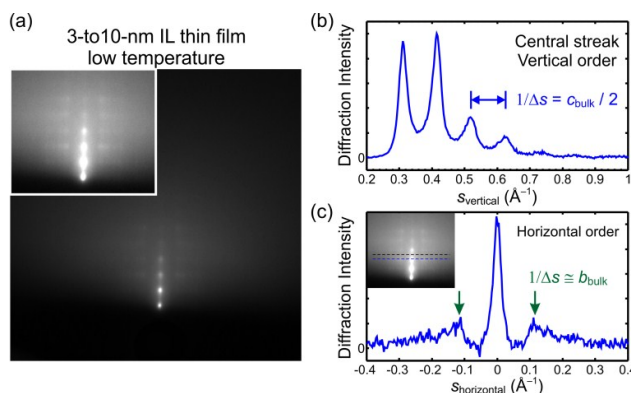


**Fig. 2.** RHEED image of the ordered IL structure on HOPG. (a) Diffractions of ultrathin IL films with a thickness of 3 to 10 nm, at the specimen temperature below the melting point ( $T < 250 \text{ K}$ ). Inset: the intensity-enhanced central region to show the weaker diffractions. (b) The intensity profile along the central streak subtracted by that of a nearby background. Multiple orders of the diffraction are apparent, indicating a vertical crystalline order in the IL film similar to the  $c$  axis of the bulk crystal. (c) The intensity profile along the horizontal direction (the blue dashed line in the inset) subtracted by that of a nearby background (the black dashed line in the inset). The green arrows indicate the first diffractions on the side streaks. The spacing signifies a horizontal order that matches with the  $b$  axis of the bulk crystal.

spacing in Fig. 2b originates from the crystalline layers of ions whose interlayer distance matches with half of the  $c$  axis of the [EMIM][Tf<sub>2</sub>N] crystal structure ( $c/2 = 9.628 \text{ \AA}$ ); the minimum horizontal spacing seen in Fig. 2c can be associated with the  $b$  axis ( $b = 8.626 \text{ \AA}$ ).<sup>19</sup> This analysis signifies that cations and anions of the IL are packed in the 3-dimensional checkerboard-type configuration following the orthorhombic structure of the bulk crystal, with the  $a$ - $b$  plane being parallel to the basal plane of the graphite substrate. Hence, it also means that the imidazolium rings are parallel, not perpendicular, to the graphene sheet. To further support such a structural determination, simulations of diffraction patterns were conducted using the kinematic scattering theory, in which the diffraction intensity is proportional to the square of the total scattered wave amplitude from all atoms,

$$I \propto \left| \sum_j f_j^{(e)}(s) \exp(-2\pi i \vec{s} \cdot \vec{r}_j) \right|^2,$$

where  $f_j^{(e)}(s)$  is the atomic scattering factor of the  $j$ -th atom as a function of  $s$  and  $\vec{r}_j$  is the atom's position. Because the  $b$  and  $c/2$  cell constants are somewhat close, we have considered the following two possibilities to explain the multiple diffractions aligned sideways: (1) the  $c$  axis perpendicular to the surface and the  $a$ - $b$  plane azimuthally rotated and averaged with respect to the substrate (Fig. S1a, ESI<sup>†</sup>), and (2) the  $b$  axis perpendicular to the surface and the  $a$ - $c$  plane azimuthally rotated and averaged (Fig. S1b). It is evident that the former structural assignment leads to all of the experimentally observed spot alignments, which match reasonably well with Fig. 2a, whereas the latter one gives a completely different result thus can be ruled out.

There are additional observations that are worth noting. First, this ordered IL structure in the 3-to-10-nm films appears over the entire specimen area in a first-order transition below 235 K, which is  $\sim 20 \text{ K}$  lower than the melting point of the bulk IL, 252~258 K, and well above the glass transition temperature

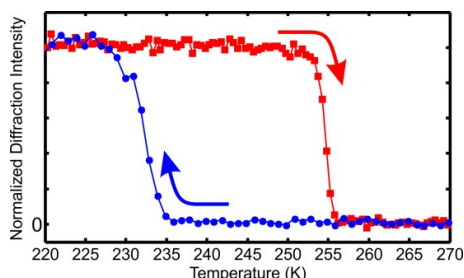


Fig. 3. Typical changes of the IL diffraction spot intensity as a function of the specimen temperature during the cooling (blue dots) and warming (red squares) cycles.

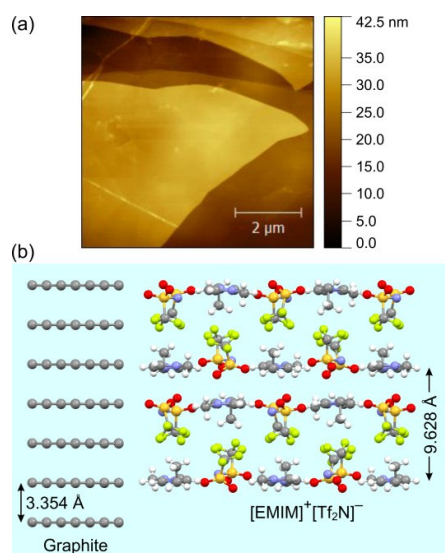


Fig. 4. The lattice-matching template effect at the IL-HOPG interface. (a) The terraced HOPG surface shown in an AFM image. (b) Comparison of the crystal structures of graphite and [EMIM][Tf<sub>2</sub>N]. It is evident that their interlayer distances are commensurate.

reported previously<sup>20, 21</sup> (Fig. 3, blue dots). Therefore, the supercooling phenomenon of [EMIM][Tf<sub>2</sub>N]<sup>19, 20</sup> is much reduced at the IL-HOPG interface, with a cooling rate of  $\sim 3$  K/min. Second, loss of the crystalline order during warming takes place at the same temperature as the melting point reported for the bulk (Fig. 3, red squares). This melting behaviour, together with the structural similarity seen in the diffraction, provides direct evidence that the 3-to-10-nm-thick IL layers are essentially bulk-like, which seems at odds with the notion that interfacial phenomena typically exhibit differences from the bulk ones and differs from a previous study of [EMIM][Tf<sub>2</sub>N] on Au(111) by helium atom scattering.<sup>22</sup> Third, evidence shows that the ordered IL structure extends toward the IL-vacuum interface for the 3-to-10-nm thick films, as the Bragg diffractions can still be seen using 10-keV electrons for probing of mostly the topmost IL layer (see ESI<sup>†</sup>).

On the other hand, we note that the IL films thinner than  $\sim 2$  nm or thicker than  $\sim 15$  nm only yield diffuse scattering images at all temperatures in the thickness-dependent experiments. The lower limit of 2 nm is close to the *c* cell constant that accommodates four checkerboard-type layers<sup>19</sup> as well as to the range of the interfacial “solid-like layers” given in molecular dynamics (MD) simulations (see below).<sup>23-25</sup>

In the case of thicker films, we observed that an additional nanometre of the IL (via a simple increase of the deposition time by 30 seconds more) can turn the diffraction results from the well-defined Bragg spots to featureless scattering. Intriguingly, no diffraction spots were seen at low temperatures from the IL deposited on the monolayer graphene surface used. The clear difference observed on the two resembling carbon substrates is marked, even though the interactions between the ions and the two surfaces are expected to be comparable.

The aforementioned observations prompt us to answer the questions why HOPG readily allows the IL to form a crystalline interfacial structure—but only within a specific thickness range—and why other substrate surfaces do not favour it.<sup>5</sup> One major difference between the HOPG and graphene surfaces is that the former is a terraced one with single- and multi-layer steps formed by atomically flat domains (Fig. 4a). We note that the *c* lattice constant of the IL is commensurate with that of graphite: the vertical distance for two checkerboard-type IL layers ( $c/2 = 9.628$  Å) and three times of the interlayer distance of graphite (3.354 Å) differ by less than 10% (Fig. 4b). Hence, our diffraction results support the molecular picture that the pronounced crystalline order of the multiple [EMIM][Tf<sub>2</sub>N] layers on HOPG originates from the lattice-matching effect throughout the film toward the IL-vacuum interface, where the surface steps and terrace of HOPG serve as a structural template to facilitate especially the vertical order in the 3-to-10-nm IL films. Energetically, the surface energy of HOPG may be reduced because of the local IL order favoured near the steps, which likely serves as the nucleation sites for the IL’s crystalline structure extended over sub-micrometre to micrometre-sized basal-plane domains. Without the solid surface confinement, however, the IL ions on graphene show no strong propensity to form ordered solid layers or nm-sized crystallites at low temperatures. This implies that the Coulombic interactions of ions alone are not sufficient for an extended structural order in ultrathin films. As a comparison, a similar lattice-matching template effect has been observed in the system of the water-HOPG interface where the intermolecular interactions—the hydrogen bonds—are also strong and the crystallization of cubic ice always takes place whether in vertical layers or in small crystallites.<sup>15</sup>

Therefore, for the interfacial IL to crystallize in a bulk-like structure, we argue that above the melting temperature the [EMIM]<sup>+</sup> cations and [Tf<sub>2</sub>N]<sup>-</sup> anions need to be arranged by a structural template and spatially adjacent to each other in the pairwise, liquid-like configuration, instead of electrical double-layer formations. Inside the template, the IL ions show bulk-like behaviours as a result of the combination of their interionic electrostatic, dispersion, hydrogen bonding, and hydrophobic interactions.<sup>19</sup> This picture is consistent with the flat ion density profiles at a distance of  $\geq 2$  nm away from uncharged graphite calculated using MD simulations, although the surface was presumed to be perfectly planar,<sup>23-25</sup> slightly bumpy artificially,<sup>26</sup> or with no more than two steps in a recent study.<sup>27</sup> The template effect for the ordered IL structure is expected to diminish as the IL film thickness increases and the

ions are further away from the terraced substrate surface.<sup>15</sup> Indeed, the disappearance of the diffraction spots caused by the deposition of additional IL layers is consistent with such an expectation as well as the observations at the IL-graphene interface. This implies that, on the molecular level, the orientations of the IL ions are possibly different at the IL-vacuum interfacial region when the film thickness is sufficiently larger than the substrate surface roughness. Nevertheless, as suggested by the MD studies,<sup>23, 25</sup> this upper interface is expected to affect little on the underneath layers ordered by the HOPG template effect.

In contrast, the lack of Bragg diffractions from very thin (<2 nm) IL films may have multiple reasons, from the structural and/or interfacial interaction viewpoints. Structurally, the basal-plane structure of graphene/graphite and the *a-b* plane of the IL checkboard-type layers do not match well. Previous AFM and MD studies suggest that the ion layering and structures of [EMIM][Tf<sub>2</sub>N] within the first 2 nm of the neutral HOPG surface are substantially different from those of the bulk.<sup>28</sup> It is also likely that, concurrently, the reduced ion mobility due to the van der Waals interaction between the IL and the graphite surface<sup>29</sup> enhances the supercooling phenomenon and consequently hinders crystallization. Based on the present study, the lattice-matching template effect may not be pronounced yet in ultrathin films to facilitate orders especially in the vertical direction. Therefore, to assess the relative importance of the aforementioned factors, it will be crucial to conduct further studies using varieties of ILs and solid substrates and also surface charges for comparison, which are underway.

In summary, RHEED has been presented as a contactless method to visualize the ion organization and layer structures at the IL-solid interfaces. Using [EMIM][Tf<sub>2</sub>N] as a prototype IL, three distinct ranges of the film thickness can be identified for the ion layering and structures on HOPG. Cations and anions within ~2 nm from the substrate surface are influenced by the interface and fail to form an extensive crystalline order at low temperatures. Above 2 nm in the 3-to-10-nm range, ions display the bulk-like structure and melting behaviours as a result of the restricted motions on the terraced HOPG surface as well as the lattice-matching template effect. Further away from the surface, such a template phenomenon subsides and the topmost ion layers fail to crystallize again, which offers evidence for a different ion organization at the IL-vacuum interface. The consistent observations seen at the IL-graphene interface further substantiate the influence of the surface topography of HOPG on the behaviours of the IL. The present study not only demonstrates the capabilities of RHEED for static structural probing of IL-solid interfaces at the collective molecular level, but also paves the way for dynamics studies using the pump-probe scheme to probe interfacial phenomena induced via photoexcitation.

### Acknowledgements

This research was supported by the R. A. Welch Foundation (Grant No. E-1860), the Donors of the American Chemical

Society Petroleum Research Fund (ACS-PRF), and the University of Houston (UH). X.H. acknowledges Dr. Herman Suit and Dr. Joan Suit for the Eby Nell McElrath Postdoctoral Fellowship. The authors acknowledge Dr. Steve Baldelli for helpful discussion and Drs. T. Randall Lee and Andrew C. Jamison for their assistance with the AFM measurements.

### Notes and references

§ Initial results indicate no bulk-like, ordered IL structure on H-terminated Si(111) and Ar<sup>+</sup>-sputtered Cu(111) and Ni(111).

§§ Given the finite energy and angular spread, the electron beam used has a transverse coherence length of the order of few tens of nm. The lack of diffraction features indicates the disorder of the ions within a lateral range of ~10 unit cells.

- 1 P. Wasserscheid and W. Keim, *Angew. Chem. Int. Ed.*, 2000, **39**, 3772-3789.
- 2 N. V. Plechkova and K. R. Seddon, *Chem. Soc. Rev.*, 2008, **37**, 123-150.
- 3 H.-P. Steinrück, *Phys. Chem. Chem. Phys.*, 2012, **14**, 5010-5029.
- 4 S. Baldelli, *J. Phys. Chem. Lett.*, 2013, **4**, 244-252.
- 5 R. Hayes, G. G. Warr and R. Atkin, *Chem. Rev.*, 2015, **115**, 6357-6426 and references therein.
- 6 M. Mezger, H. Schroder, H. Reichert, S. Schramm, J. S. Okasinski, S. Schöder, V. Honkimäki, M. Deutsch, B. M. Ocko, J. Ralston, M. Rohwerder, M. Stratmann and H. Dosch, *Science*, 2008, **322**, 424-428.
- 7 L. Tamam, B. M. Ocko, H. Reichert and M. Deutsch, *Phys. Rev. Lett.*, 2011, **106**, 197801.
- 8 Z. Brkljača, M. Klimczak, Z. Miličević, M. Weisser, N. Taccardi, P. Wasserscheid, D. M. Smith, A. Magerl and A.-S. Smith, *J. Phys. Chem. Lett.*, 2015, **6**, 549-555.
- 9 T. Cremer, M. Killian, J. M. Gottfried, N. Paape, P. Wasserscheid, F. Maier and H.-P. Steinrück, *ChemPhysChem*, 2008, **9**, 2185-2190.
- 10 S. Bovio, A. Podestà, C. Lenardi and P. Milani, *J. Phys. Chem. B*, 2009, **113**, 6600-6603.
- 11 Y.-X. Zhong, J.-W. Yan, M.-G. Li, X. Zhang, D.-W. He and B.-W. Mao, *J. Am. Chem. Soc.*, 2014, **136**, 14682-14685.
- 12 T. Waldmann, H.-H. Huang, H. E. Hoster, O. Höfft, F. Endres and R. J. Behm, *ChemPhysChem*, 2011, **12**, 2565-2567.
- 13 R. Foulston, S. Gangopadhyay, C. Chiu, P. Moriarty and R. G. Jones, *Phys. Chem. Chem. Phys.*, 2012, **14**, 6054-6066.
- 14 D.-S. Yang, N. Gedik and A. H. Zewail, *J. Phys. Chem. C*, 2007, **111**, 4889-4919.
- 15 D.-S. Yang and A. H. Zewail, *Proc. Natl. Acad. Sci. U.S.A.*, 2009, **106**, 4122-4126.
- 16 R. Henderson, *Q. Rev. Biophys.*, 1995, **28**, 171-193.
- 17 K. J. Baranyai, G. B. Deacon, D. R. MacFarlane, J. M. Pringle and J. L. Scott, *Aust. J. Chem.*, 2004, **57**, 145-147.
- 18 J. P. Armstrong, C. Hurst, R. G. Jones, P. Licence, K. R. J. Lovelock, C. J. Satterley and I. J. Villar-Garcia, *Phys. Chem. Chem. Phys.*, 2007, **9**, 982-990.
- 19 A. R. Choudhury, N. Winterton, A. Steiner, A. I. Cooper and K. A. Johnson, *CrystEngComm*, 2006, **8**, 742-745.
- 20 A. Noda, K. Hayamizu and M. Watanabe, *J. Phys. Chem. B*, 2001, **105**, 4603-4610.
- 21 S. J. Zhang, N. Sun, X. Z. He, X. M. Lu and X. P. Zhang, *J. Phys. Chem. Ref. Data*, 2006, **35**, 1475-1517.
- 22 E. M. McIntosh, J. Ellis, A. P. Jardine, P. Licence, R. G. Jones and W. Allison, *Chem. Sci.*, 2014, **5**, 667-676.
- 23 M. L. Sha, F. C. Zhang, G. Z. Wu, H. P. Fang, C. L. Wang, S. M. Chen, Y. Zhang and J. Hu, *J. Chem. Phys.*, 2008, **128**, 134504.

- 24 M. V. Fedorov and R. M. Lynden-Bell, *Phys. Chem. Chem. Phys.*, 2012, **14**, 2552-2556.
- 25 Y. L. Wang, A. Laaksonen and Z. Y. Lu, *Phys. Chem. Chem. Phys.*, 2013, **15**, 13559-13569.
- 26 J. Vatamanu, L. L. Cao, O. Borodin, D. Bedrov and G. D. Smith, *J. Phys. Chem. Lett.*, 2011, **2**, 2267-2272.
- 27 G. Feng, S. Li, W. Zhao and P. T. Cummings, *AIChE J.*, 2015, **61**, 3022-3028.
- 28 J. M. Black, D. Walters, A. Labuda, G. Feng, P. C. Hillesheim, S. Dai, P. T. Cummings, S. V. Kalinin, R. Proksch and N. Balke, *Nano Lett.*, 2013, **13**, 5954-5960.
- 29 Q. A. Dou, M. L. Sha, H. Y. Fu and G. Z. Wu, *ChemPhysChem*, 2010, **11**, 2438-2443.